Toxicology in Vitro 52 (2018) 384–398

Contents lists available at ScienceDirect

Toxicology in Vitro

journal homepage: www.elsevier.com/locate/toxinvit

Delivery efficiencies of constituents of combustion-derived aerosols across the air-liquid interface during *in vitro* exposures☆

Sandro Steiner*, Pierrick Diana, Eric Dossin, Philippe Guy, Grégory Vuillaume, Athanasios Kondylis, Shoaib Majeed, Stefan Frentzel, Julia Hoeng

PMI R&D, Philip Morris Products S.A., Quai Jeanrenaud 5, 2000, Neuchatel, Switzerland

ARTICLE INFO

Keywords:
In vitro exposure
Cigarette smoke exposure
Aerosol dose
Aerosol
Combustion derived aerosol

ABSTRACT

In vitro aerosol exposure of epithelial cells grown at the air-liquid interface is an experimental methodology widely used in respiratory toxicology. The exposure depends to a large part on the physicochemical properties of individual aerosol constituents, as they determine the transfer kinetics from the aerosol into the cells.

We characterized the transfer of 70 cigarette smoke constituents from the smoke into aqueous samples exposed in the Vitrocell® 24/48 aerosol exposure system. The amounts of these compounds in the applied smoke were determined by trapping whole smoke in *N,N*-dimethylformamide and then compared with their amounts in smoke-exposed, phosphate-buffered saline, yielding compound specific delivery efficiencies.

Delivery efficiencies of different smoke constituents differed by up to five orders of magnitude, which indicates that the composition of the applied smoke is not necessarily representative for the delivered smoke. Therefore, dose metrics for *in vitro* exposure experiments should, if possible, be based on delivered and not applied doses. A comparison to literature on *in vivo* smoke retention in the respiratory tract indicated that the same applies for smoke retention in the respiratory tract.

1. Background

Since the introduction of the 3R principles (replacement, reduction, and refinement of animal experiments) in the late 1950s (Burch and Russel, 1959), *in vitro* methods in biology have gained widespread acceptance and represent an indispensable tool in drug development and consumer product assessment.

In the field of inhalation toxicology research, complex, three-dimensional, organotypic cell cultures have been developed that mimic the physiology of human airway epithelia (Shamir and Ewald, 2014). Exposures of these advanced cellular models to aerosols or gases can be conducted at the air-liquid interface, with the test agent administered in gaseous or aerosolized form (Muller et al., 2012; Paur et al., 2011; Li, 2016).

Although it is the optimal exposure mode from a biological/toxicological standpoint, exposure at the air-liquid interface represents a considerable methodological challenge. First, it requires reliable methods for aerosol generation (*e.g.*, smoking machines and standardized smoking protocols (Thorne and Adamson, 2013)) and application (*i.e.*, aerosol exposure systems (Paur et al., 2011; Thorne and Adamson, 2013; Breheny et al., 2014; Muller et al., 2011; Fröhlich et al., 2013)). Second, aerosol constituents must be transferred from the aerosol into the liquid lining of a cell culture to exert an effect on the biological test system. The physical mechanisms underlying this transfer typically differ for small and large particles, for particles and volatile compounds, and for volatile compounds of different vapor pressure, polarity, and molecular mass (Pankow, 2001) (Fig. 1). In commonly used exposure systems (Thorne and Adamson, 2013; Breheny et al., 2014; Muller et al., 2011; Fröhlich et al., 2013; Paur et al., 2008), the transfer of large particles—and of chemical compounds adsorbed to or condensed on their surfaces or contained in their cores—is driven mainly by gravitation (and to a limited extent by inertial impaction). Brownian motion becomes more important with decreasing particle size (Von der Weiden et al., 2009), whereas the transfer of gaseous constituents relies primarily on diffusion (Pankow, 2001; Tippe et al., 2002; Davidovits et al., 2006). Once transferred into the liquid, aerosol constituents may return to the gas phase. While this does not occur with solid, insoluble particles and is of limited relevance for compounds of low vapor

☆ All authors are employees of Philip Morris International. This work was funded by Philip Morris International R&D.
* Corresponding author.
E-mail addresses: Sandro.Steiner@pmi.com (S. Steiner), Pierrick.Diana@contracted.pmi.com (P. Diana), Eric.Dossin@pmi.com (E. Dossin), PhilippeAlexandre.Guy@pmi.com (P. Guy), Gregory.Vuillaume@pmi.com (G. Vuillaume), Athanasios.Kondylis@pmi.com (A. Kondylis), Shoaib.Majeed@pmi.com (S. Majeed), Stefan.Frentzel@pmi.com (S. Frentzel), Julia.Hoeng@pmi.com (J. Hoeng).

https://doi.org/10.1016/j.tiv.2018.06.024
Received 19 March 2018; Received in revised form 20 June 2018; Accepted 29 June 2018
Available online 09 July 2018

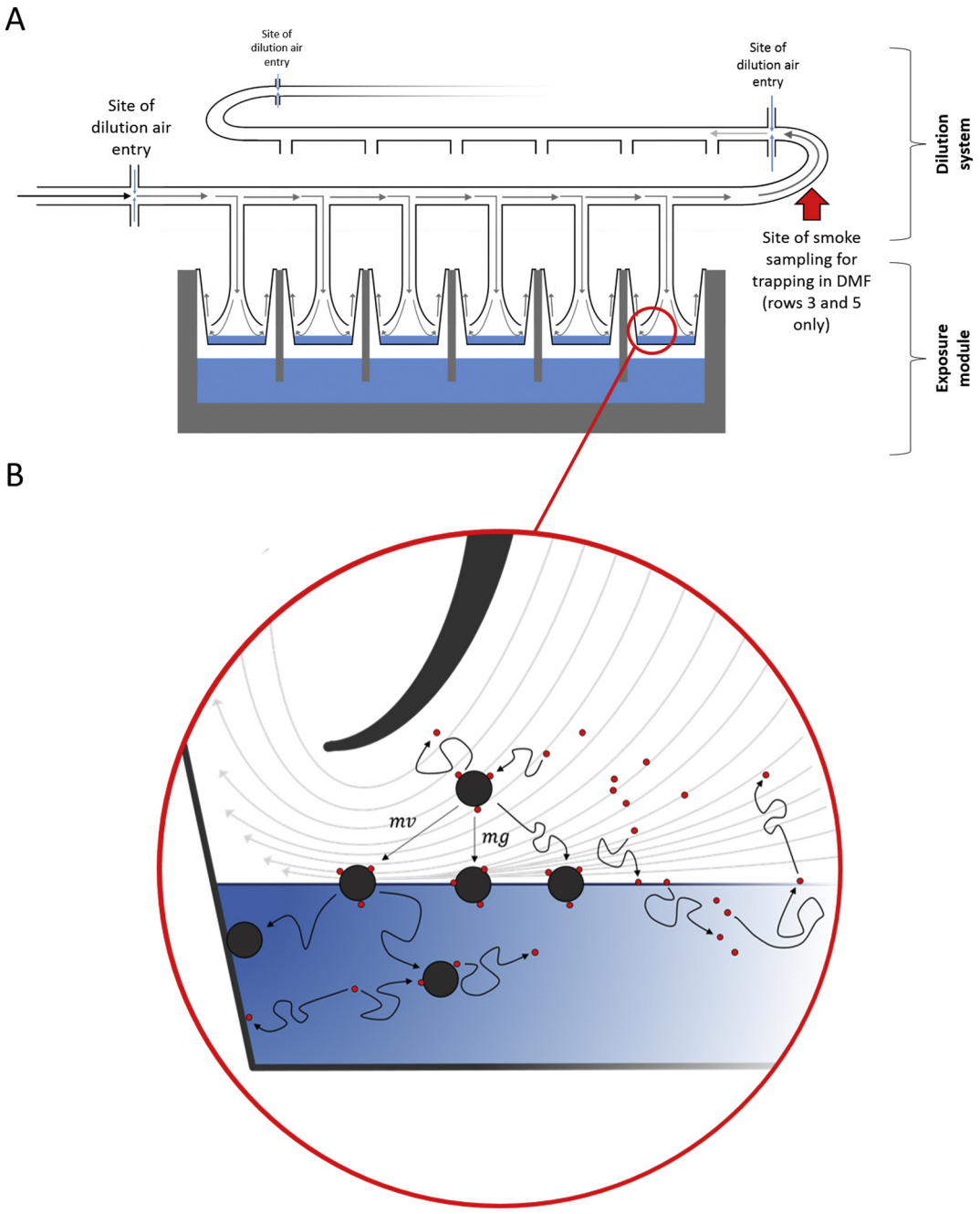

Fig. 1. A) Schematic representation of the VC24/48 system. Shown above is the dilution module comprising the dilution rows (top; only one of the eight serially connected rows is shown in full) and the exposure trumpets projecting into the exposure chambers in the exposure module (bottom), where the biological test systems are located during *in vitro* aerosol exposures. In the exposure module, the PBS containing cell culture inserts are shown. Points of dilution air access are shown and one point at which smoke was collected for trapping in DMF is indicated by a red arrow. B) Main processes by which aerosol constituents are transferred into an exposed liquid. Red spheres represent (semi-) volatile aerosol constituents, black spheres represent particles. The flow pattern in the exposure chamber is indicated by light gray, curved arrows. Particles deposit on the liquid surface by either sedimentation (mg), inertial impact (mv), or diffusion (irregularly shaped arrows), and, depending on hydrophilicity and density, may subsequently enter the bulk liquid. Liquid or soluble particles may dissolve in the liquid surface or the bulk liquid (not shown). (Semi-) volatile aerosol constituents may be present in their free form and/or adsorbed to/condensed on particle surfaces. In the latter case, the (semi-) volatile aerosol constituents follow the fate of the particles and may desorb from the particles once in contact with the liquid. In their free form, the constituents reach the liquid interface by diffusion and may subsequently be dissolved in the bulk liquid or adsorb to particle surfaces again. *Re*-evaporation may occur, depending on factors such as solubility in the liquid and vapor pressure. Both particles and (semi-) volatile compounds may adsorb to the surfaces of the cell culture inserts, decreasing their effective concentration in the liquid.

pressure, it may be relevant for volatile aerosol constituents, as they may reach equilibrium concentrations (Atkin and de Paula, 2006). The net transfer of a given aerosol constituent from the aerosol across a liquid surface into a bulk liquid is, consequently, a function of the geometry of the exposure chamber, the aerosol flow pattern, the temperature and pressure in the exposure chamber, the compound's partitioning between the gas and particulate aerosol fraction and its chemical potential in the liquid and the aerosol.

Given the complexity of this transfer process and the number of parameters involved, the process may result in considerable differences

between the composition of the applied aerosol and the aerosol fraction that reaches the liquid lining of a cell culture. This can be understood as the conversion of the applied aerosol dose to the delivered aerosol dose. The applied aerosol dose is the sum of all aerosol constituents present in the aerosol, and the delivered aerosol dose is the sum of all aerosol constituents that reach across the liquid lining of a cell culture during exposure (Teeguarden et al., 2006).

For methodological reasons, *in vitro* aerosol exposures are commonly characterized by the composition and concentration of the aerosol originally generated and the exposure duration, but not by the delivered aerosol fraction. In theory, the rate at which aerosol constituents are delivered across a liquid surface could be predicted, as the underlying particle deposition efficiencies and diffusion fluxes can be calculated when the composition of the aerosol, the partitioning of its constituents between the particulate and the gaseous phases, and the mass accommodation coefficients for the gaseous compounds are known. These parameters are, however, in most cases unavailable for the majority of aerosol constituents and even when they are available, they are not commonly known for compound mixtures (Pankow, 2001; Von der Weiden et al., 2009; Davidovits et al., 2006).

We pursued an experimental approach to describe the transfer of various constituents of a complex, combustion-derived aerosol across an aqueous surface under conditions commonly applied during *in vitro* aerosol exposures. The presence of various chemical compounds in the smoke and in the fraction of the smoke transferred across a liquid surface was determined. From these two values, compound-specific delivery efficiencies were derived. These dimensionless values offer a simple measure for describing the conversion from an applied to a delivered dose and are therefore a valuable tool for *in vitro* dose metrics. They can be considered as describing physical processes at phase boundaries which, as long as relevant parameters such as temperature or pressure are kept stable, are of limited specificity to the exact experimental design (Atkin and de Paula, 2006), and may hence be used for estimating dose delivery for aerosols other than the one used in this work and may even allow prediction of the delivery efficiencies of compounds not covered here.

As a representative source of smoke, we selected the 3R4F reference cigarette, a highly standardized test product from which smoke can be generated reproducibly. Cigarette smoke is a suitable model aerosol for this work, because its high complexity (Pankow, 2001; Perfetti and Rodgman, 2011) offers insights into the effects of individual compound characteristics on delivery and because, despite its high complexity, its chemical composition is comparatively well-described (Perfetti and Rodgman, 2011; Forehand et al., 2000; Eldridge et al., 2015; Paschke et al., 2014). Additionally, as many cigarette smoke constituents also occur in other combustion-derived aerosols that are environmentally abundant and of toxicological relevance (Sarigiannis et al., 2011; Shahir et al., 2015; Kumar et al., 2011; Schauer et al., 2002a; Khalili et al., 1995; Schauer et al., 2002b; Schauer et al., 1999; Schauer et al., 2001), the conclusions drawn from this work have a broader validity and are not exclusive to cigarette smoke.

To assure the controlled and reproducible application of the smoke, we conducted the exposures in the Vitrocell® 24/48 aerosol exposure system (VC24/48, Vitrocell Systems GmbH, Waldkirch, Germany), which has been shown to reliably provide a controlled and stable environment for smoke exposures *in vitro* (Majeed et al., 2014; Steiner et al., 2017a). Phosphate-buffered saline (PBS) was selected as a surrogate for the surface of cell cultures which, irrespective of the exact cell type, are commonly covered by at least a thin film of an aqueous matrix. With respect to pH and salt concentrations, PBS provides a good model for such liquid films, but due to its low complexity, it is not expected to interact chemically with delivered aerosol constituents nor to interfere with their quantification.

2. Methods

2.1. Smoke generation

3R4F reference cigarettes, obtained from the University of Kentucky (Lexington, KY, USA) were conditioned according to ISO guidelines (48 h at 22 ± 1 °C and 60 ± 3% relative humidity). For aerosol generation, the cigarettes were smoked in a 30-port carousel rotary smoking machine (SM2000, Philip Morris International) under a modified Health Canada regimen (two 55-mL puffs per cigarette per minute; a bell-shaped puff profile with 2-s aspiration and 8-s emission). The smoke was delivered to the VC24/48 system at room temperature through 0.8 m long fluoroelastomer tubing (ISO-Versinic®, Saint-Gobain, Courbevoie, France).

2.2. VC24/48 system setup and exposures

The working principle of the VC24/48 system is summarized in Fig. 1. The test aerosol passes through the system *via* a dilution module located on top of the exposure module. The exposure module provides 48 exposure chambers, which are grouped into eight rows of six replicate positions. Upstream of each row, the aerosol in the dilution module can be diluted with clean air, resulting in a total of eight dilutions that can be tested simultaneously (one per row). Under standard operating conditions, only seven dilutions are tested, while the eighth row is used for negative control exposure to clean air only. The aerosol passing through the dilution module is sampled by negative pressure into exposure trumpets, which project into the exposure chambers in the exposure module and generate a stagnation flow condition over the biological test system. More information on the VC24/48 system can be found on the manufacturer's website (www.vitrocell.com, n.d.).

The dilution air was brought to a temperature of 37 °C and a relative humidity of 60% and supplied to the dilution module with cumulative volume flow rates of 0.1, 0.2, 0.5, 1, 1.5, 2, and 3 L/min applied to rows 1–7, corresponding to a dilution of the applied smoke to 81%, 67%, 45%, 29%, 22%, 17%, and 12%, respectively. Row 8 was reserved for control exposures to clean air. The volume flow rate to the exposure chambers was set to 2 mL/min for all positions. The whole system was maintained at a temperature of 37 °C throughout the entire procedure.

For exposures of PBS samples, ThinCert™ cell culture inserts (24-well format, transparent insert membrane, 0.4-µm pore diameter; Greiner Bio-One, Kremsmünster, Austria) containing 100 µL Dulbecco's PBS (Sigma-Aldrich, St. Louis, MO, USA) were placed into each position in the cultivation base module. Leakage of PBS through the pores in the membrane did not occur as confirmed visually and volumetrically. The six positions of each exposure row in the cultivation base module are connected, but these connections were interrupted by adding PBS to a level where it covered the connection, but did not get into contact with the cell culture inserts). The PBS samples were exposed to smoke generated from 10 3R4F cigarettes (11 puffs per cigarette). To account for system memory effects, the first exposure run on each day of exposure was conducted with clean air instead of smoke. These blank runs were conducted for 28 min (corresponding to the time during which 110 puffs are generated by the smoking machine), with PBS-loaded cell culture inserts placed in rows 1 and 7 only.

Immediately after exposure, 80-µL aliquots of the exposed PBS samples were collected from each cell culture insert. The samples were pooled row-wise and stored at −80 °C until chemical analyses were performed. PBS exposures were conducted in three to four replicates generated on different days.

2.3. Smoke trapping in N,N-Dimethylformamide (DMF)

To determine the composition of the smoke used for exposure, smoke leaving the VC24/48 dilution system was trapped in three serially connected glass impingers, each containing 5 mL DMF (≥99%,

Sigma-Aldrich). DMF has been shown to be an effective solvent for various polar and non-polar organic compounds. Its relatively low melting point allows trapping at low temperatures, which increases the trapping efficiency of volatile compounds (Johansen and Wendelboe, 1981; Harper, 2000), while its high boiling point reduces its impact on the chromatography. The impingers were cooled to −50 ± 5 °C by immersion in a dry ice-isopropanol mixture. As frozen, condensed water tended to clog the impinger needles over time at this temperature, smoke from only two cigarettes was collected (22 puffs). An effect of smoke dilution *per se* on the overall mass of trapped smoke constituents was not expected, as the complete smoke volume passed the impingers, irrespective of the dilution. However, with increased smoke dilution, the smoke traveled a longer path through the system. Therefore, detectably higher losses on internal system surfaces could have affected the trapped masses of smoke constituents. To obtain an estimate of the relevance of this effect, two dilutions were tested: smoke was trapped downstream of row 3 (1 L/min cumulative dilution air flow rate, 45% smoke) and downstream of row 5 (2 L/min cumulative dilution air flow rate, 22% smoke). At each concentration, DMF trapping was repeated six to eight times on different days.

Following trapping, the DMF contained in the three impingers was pooled (for a total sample volume of 15 mL) and stored at −80 °C until chemical analyses were performed. Blank runs using clean air instead of smoke were performed to assess system memory effects.

2.4. Confirmation of the trapping efficiency in DMF

The trapping efficiency in DMF was confirmed in separate experiments by analyzing the compounds in the DMF obtained individually from four serially installed impingers under otherwise identical settings. Although it is only the case at equilibrium conditions and does not apply strictly to particles, the partition coefficients describing the distribution between the smoke and DMF are expected to be constant for each smoke constituent, irrespective of the total amount of the constituent in the smoke (Adam et al., 2009). Furthermore, as mass conservation applies, the relative decrease in the mass of a given smoke constituent trapped in DMF in two adjacent impingers equals its relative depletion from the smoke when passing through an impinger. The ratio between the a compound's relative response (RR) (the peak area (obtained by mass-spectrometry) of detected compounds relative to the peak area of the internal standard benzene-d_6) measured in the DMF obtained from impinger n and from impinger n − 1 is therefore equal to its breakthrough rate (the fraction of the total mass of the constituent present in smoke that evades trapping in the solvent).

We used these breakthrough rates for deriving an estimate of how well smoke composition was described during our experiments by calculating trapping efficiencies (E_{trap}, Eq. (1)). The breakthrough rates determined from the experiments using four impingers were averaged for this purpose. This was only performed for the more volatile compounds (Method 1, described below), as trapping at −50 °C can be assumed to be quantitative for compounds of low vapor pressure and only at a smoke concentration of 22% (2 L/min air flow).

$$E_{trap} = 1 - \left(mean \left(\frac{RR_{(impinger\ n)}}{RR_{(impinger\ n-1)}} \right) \right)^3 \quad (1)$$

2.5. Analytical procedures

There is no consensus on the most appropriate method to assess tobacco smoke dosimetry. Some techniques look at specific tobacco smoke markers, such as nicotine and solanesol in the particulate phase or carbon monoxide in the gas phase, while others quantify smoke in larger groups of chemicals (Scian et al., 2009; Kaur et al., 2011; Kaur et al., 2010). In order to cover a broad spectrum of smoke constituents, we applied five different analytical methods to characterize the gas phase and the particulate phase. The five methods were used for analyzing both PBS and DMF samples. Matrix effects of either of the two solvents could not be detected (data not shown). The five methods are described in detail in the Supplemental Information. Method 1, headspace injection gas chromatography coupled to high-resolution mass spectroscopy (GC-HRMS), was applied in both targeted and non-targeted mode, yielding absolute concentrations for a selection of six representative compounds and RRs only for the others. Methods 2 to 5 were only applied in targeted mode (Method 2, liquid chromatography coupled to tandem mass spectrometry (LC-MS/MS); Method 3, liquid-liquid extraction followed by liquid chromatography coupled to mass spectrometry; Method 4, LC-MS/MS quantification of compounds not targeted by Method 2; Method 5, liquid-liquid extraction followed by gas chromatography coupled to mass spectroscopy). In total, 15 compounds were covered by Methods 2 to 5. Absolute quantification was thereby included primarily to obtain an estimate of absolute dosing and of the reliability of our analytical approaches in comparison with published values in the literature. When calculating delivery efficiencies, dimensionless values are obtained, *i.e.* absolute and relative quantification are equivalent.

2.6. Data processing

Absolute quantification data were converted to mass per cigarette (for DMF samples) and to mass per cigarette per cell culture insert (for PBS samples). Analogously, the RRs obtained from non-targeted analyses were converted to RR per cigarette and to RR per cigarette per cell culture insert.

Absolute concentrations were used directly to describe the composition of the smoke and the delivery of individual smoke constituents.

RRs obtained for different smoke constituents cannot be compared to each other (*i.e.*, the relative abundancies of different smoke constituents in a PBS or a DMF sample cannot be derived from RRs). However, a direct comparison of the RRs obtained from PBS *and* DMF samples for *one* given compound is possible and allows the derivation of compound-specific delivery efficiencies (E_{del}, Eq. (2)).

$$E_{del} = \frac{\frac{RR_{(PBS)}}{Cigarette\ and\ insert}}{\frac{RR_{(DMF)}}{Cigarette}} \times \frac{100}{F_v} \quad (2)$$

where

$$F_v = \frac{Exposure\ trumpet\ volume\ flow\ rate\ (2mL/min)}{Total\ volume\ flow\ rate\ within\ VC24/48\ system\ (puff\ emission + dilution\ air)} \quad (3)$$

Compound-specific delivery efficiencies describe the percentage of molecules transferred to PBS samples relative to the total amount reaching the exposure chambers, as determined by trapping in DMF. The sampled volume fraction (F_v, Eq. (3)) is a correction factor required to adjust for smoke dilution and sampling into the exposure trumpets within the VC24/48 system. It refers to the fraction of smoke volume supplied to the VC24/48 system (emitted by the pump after puff generation) that is sampled into an individual exposure trumpet and reaches the exposure chamber. The sampled volume fraction is based on the assumptions that the sampling of smoke into the exposure trumpets is ideal and equal for all smoke constituents.

Using the analogous procedure, but using calculated concentration values instead of the RRs in Eq. (2), delivery efficiencies were also derived from the targeted analyses.

3. Results

3.1. Absolute quantification: smoke composition from targeted quantitative analyses

Table 1 lists the mean, standard deviation, and number of measurements performed for each quantified compound per cigarette and delivered per cell culture insert. The amounts of different compounds detected in the smoke varied by several orders of magnitude and, as only a small part of the total smoke was sampled into the exposure trumpets, were much higher than the amounts ultimately transferred to the PBS. An effect of smoke dilution in the VC24/48 system was clearly visible but not reflected quantitatively in the delivery: The 6.7-fold decrease in concentration when diluting the smoke from 81% to 12% resulted in a 3–30-fold decreased delivery, depending on the smoke constituent under consideration (benzo[*a*]pyrene, pyrene, phenanthrene, and naphthalene showed no consistent response to dilution, which we considered the consequence of the overall low presence of these polycyclic aromatic hydrocarbons in the smoke, the low absorption into PBS, and the accordingly low accuracy of the quantification data).

Fig. 2 shows that the contribution of the individual compounds relative to their total mass differed between applied smoke (the smoke in the dilution system) and the delivered smoke (the smoke fraction found in the exposed PBS samples): For example, nicotine and solanesol accounted for roughly 33% and 18% of the cumulative mass of the quantified constituents in the applied smoke, while their mean contributions to the mass delivered to PBS were 46% and 0.07%, respectively.

3.2. Smoke composition from non-targeted analyses: detected and identified compounds

In the generated DMF and PBS samples, we unambiguously identified and confirmed 48 additional compounds with our compound database (Dossin et al., 2016) and calculated their delivery efficiencies according to Eq. (2). Although these compounds were detected exclusively by GC-HRMS (Method 1 is optimized for the volatile and semi-volatile spectrum of smoke constituents), they exhibit a wide range of physicochemical and structural properties.

3.3. Compound-specific delivery efficiencies

Altogether, 70 compounds could be monitored in both DMF and PBS samples. Delivery efficiencies were calculated for each compound and for each applied smoke dilution according to Eqs. (2) and (3). Table 2 lists the obtained values. These delivery efficiencies ranged from 0 (benzo[*a*]pyrene at several smoke concentrations) to 124% (anabasine at a smoke concentration of 67%). Delivery efficiencies of 0 are most likely due to the limited sensitivity of the analytical methods (*i.e.*, the presence of trace amounts lower than the detection limit of the analytical instruments cannot be ruled out). Delivery efficiencies above 100% are not physically or chemically possible and therefore must be attributed to analytical variation and/or variations in the smoke composition between individual smoke generation runs. They are interpreted as a delivery efficiency close to or equal to 100%.

Because of the correction for the sampled volume fraction in Eq. (2), delivery efficiencies were expected to be independent of the smoke dilution. They were, however, commonly found to increase slightly with smoke concentration, to peak at 67% smoke, and to decline at 81% smoke. Based on previous work (Majeed et al., 2014; Steiner et al., 2017b), we consider this phenomenon primarily to be the result of deviations from the ideal internal smoke sampling in the VC24/48 system, although we cannot rule out an effect of changed gas-vapor partitioning in the smoke. As there is no clear explanation for the changes in the delivery efficiencies at high smoke concentrations, we focused subsequent analyses on smoke concentrations lower than 45%.

3.4. Comparison of in vitro delivery efficiencies to in vivo retention rates

Table 3 displays the retention rates (the percent of the mass of a given smoke constituents that is retained in the lungs, relative to the mass that was inhaled) of a number of smoke constituents *in vivo* and associates them with the *in vitro* delivery efficiencies. Considering, for example, the compound pair nicotine (as a reference compound) and toluene, the ratio between the *in vivo* retention of the two is 1.16 (using the means of all *in vivo* values listed in Table 3). This indicates that the *in vivo* retention of toluene is only slightly higher than that of nicotine, and that overall the compounds are present in roughly the same relative amounts in the inhaled smoke and in the smoke fraction retained in the lung. In contrast, the delivery efficiency of nicotine *in vitro* is roughly 500 times greater than that of toluene. Note that for toluene (with nicotine as the reference compound), the discrepancy between *in vitro* absorption and *in vivo* retention is comparably large. For 14 out of the 20 listed compounds, the same calculations yielded ratios far below 100, for 8 of the compounds even below 2.

3.5. Trapping efficiency in DMF and the effect of smoke concentration

The trapping efficiencies in DMF obtained using Eq. (1) ranged from 22% (1,3-butadiene) to 99.99% (1-methyl-1-H-pyrrole). Across all detected compounds, the first, second, and third quartiles were localized at 95.2%, 98.7%, and 99.5%. This indicates that for the majority of detected compounds, the trapping in DMF was quantitative. This is of relevance for calculating delivery efficiencies, as a suboptimal trapping efficiency of a given compound will result in the underestimation of its concentration in the smoke and consequently in the overestimation of its delivery efficiency to PBS. However, multiplication by the trapping efficiency allows us to correct compound-specific delivery efficiencies. Values corrected in this way are included in Table 2.

The trapping efficiency in DMF was confirmed further by comparing the smoke composition data derived from the DMF samples to literature values on 3R4F smoke composition (with smoke generation under identical or similar conditions) (Perfetti and Rodgman, 2011; Eldridge et al., 2015; Liu et al., 2010; Bodnar et al., 2012; Purkis et al., 2012; Marcilla et al., 2014). The values were in agreement for volatile smoke constituents, whereas we commonly measured lower yields for compounds of low vapor pressure. This was in line with our expectations, as losses in the VC24/48 system would result in lower yields and primarily affect the values of compounds of low vapor pressure. Carbonyl compounds, although commonly exhibiting high vapor pressure, were also detected in lower amounts than predicted by the literature. This can be attributed to the fact that we did not perform a derivatization as commonly recommended for the reliable quantification of carbonyl compounds (*e.g.*, using 2,4-dinitrophenylhydrazine (Leonard and Kiefer, 1966; Dong and Moldoveanu, 2004). The derivatization was omitted to avoid increasing the number of analytical methods employed). It cannot be ruled out that evaporation of the volatile carbonyl compounds from the samples (before sample freezing or during sample thawing) additionally decreased their concentrations in the samples, although this is not supported by the good agreement with the literature obtained for other volatile compounds.

An effect of the smoke concentration on trapping in DMF could not be detected. The values obtained from 22% and 45% smoke were therefore averaged and considered descriptive for the total masses of smoke constituents per cigarette or per puff at all smoke concentrations.

3.6. Control exposures

PBS samples exposed to clean air in row 8 of the VC24/48 system (exposures conducted simultaneously with smoke exposures in rows 1 to 7) did not contain detectable amounts of smoke constituents (data

Table 1
Quantification of 22 smoke constituents. 'Trapped in DMF' refers to the quantification in the dilution system of the VC24/48 and is expressed in ng/per cigarette (applied dose). 'Delivered to PBS' refers to the quantification in exposed PBS samples (delivered dose) and is expressed in ng/cigarette/exposed sample. Average values were obtained from 12 to 23 samples (for DMF trapping) or 3 to 4 samples (for exposed PBS). n* lists the number of samples in which the concentrations were below the lower limit of quantification (LLoQ). If concentrations were below LLoQ, a value of 0.5 × LLoQ was used for calulating averages.

Compound	Trapped in DMF (ng/cigarette)			Delivered to PBS at specified smoke concentrations (ng/cigarette/insert)																			
				12%			17%			22%			29%			45%			67%			81%		
	AVG ± SD	n	n*	AVG ± SD	n	n*	AVG ± SD	n	n*	AVG ± SD	n	n*	AVG ± SD	n	n*	AVG ± SD	n	n*	AVG ± SD	n	n*	AVG ± SD	n	n*
2,3-Pentanedione	34,400 ± 11,700	23	2	5.6 ± 1.4	4	0	8.4 ± 1.9	4	0	10.4 ± 1.6	4	0	16.3 ± 5.3	4	0	33.3 ± 11.2	4	0	61.3 ± 15.4	4	0	53.9 ± 16.4	4	0
3-Ethenylpyridine	161,000 ± 44,200	12	0	24 ± 5	3	0	22 ± 13	3	0	35 ± 19	3	0	54 ± 20	3	0	135 ± 16	3	0	377 ± 21	3	0	434 ± 12	3	0
Anabasine	1120 ± 290	12	5	0.2 ± 0.1	3	3	0.4 ± 0.1	3	3	0.6 ± 0.2	3	1	0.9 ± 0.2	3	0	2.4 ± 0.2	3	0	4.5 ± 0.2	3	0	4.3 ± 0.4	3	0
Anatabine	3920 ± 960	12	0	0.8 ± 0.1	3	0	1.2 ± 0.0	3	0	1.7 ± 0.1	3	0	2.5 ± 0.1	3	0	5.6 ± 0.5	3	0	10.7 ± 0.4	3	0	11.0 ± 0.7	3	0
Benzene	108,300 ± 14,600	23	0	0.03 ± 0.00	4	2	0.04 ± 0.01	4	1	0.05 ± 0.01	4	0	0.08 ± 0.01	4	0	0.14 ± 0.02	4	0	0.27 ± 0.04	4	0	0.30 ± 0.04	4	0
Benzo[*a*]pyrene	13 ± 3	12	0	0 ± 0	3	3	0 ± 0	3	3	0 ± 0	3	3	0 ± 0	3	3	0.0003 ± 0.0005	3	3	0 ± 0	3	3	0.0006 ± 0.001	3	3
Diacetyl	188,100 ± 28,200	23	0	53 ± 32	4	1	69 ± 29	4	1	74 ± 37	4	0	132 ± 30	4	0	258 ± 23	4	0	441 ± 30	4	0	369 ± 112	4	0
Fluorene	118 ± 45	12	0	0.0009 ± 0.0006	3	3	0.0014 ± 0.0025	3	2	0.0035 ± 0.0031	3	2	0.0049 ± 0.0045	3	1	0.0103 ± 0.0033	3	0	0.0208 ± 0.0059	3	0	0.0197 ± 0.0055	3	0
Isobutyraldehyde	60,200 ± 6730	23	0	2.3 ± 1.1	4	1	3.2 ± 1.2	4	1	4.1 ± 1.4	4	0	6.4 ± 1.3	4	0	12.4 ± 1.9	4	0	24.9 ± 3.2	4	0	25.2 ± 3.3	4	0
Isovaleraldehyde	32,300 ± 4490	23	0	1.3 ± 0.3	4	3	1.6 ± 0.3	4	3	1.9 ± 0.3	4	1	2.8 ± 0.4	4	0	5.0 ± 0.6	4	0	9.7 ± 0.7	4	0	10.4 ± 0.5	4	0
Naphthalene	78 ± 61	12	0	0 ± 0.0001	3	3	0.0003 ± 0.0005	3	3	0 ± 0	3	3	0.008 ± 0.0037	3	3	0.0316 ± 0.0224	3	1	0.0362 ± 0.0264	3	1	0.0303 ± 0.0397	3	2
Nicotine	507,300 ± 109,000	12	0	75 ± 19	3	0	70 ± 43	3	0	106 ± 61	3	0	173 ± 67	3	0	453 ± 35	3	0	1447 ± 86	3	0	1569 ± 143	3	0
N-Nitrosoanabasine	21 ± 4	12	0	0.001 ± 0.000	3	3	0.002 ± 0.000	3	0	0.003 ± 0.000	3	0	0.004 ± 0.000	3	0	0.012 ± 0.001	3	0	0.025 ± 0.003	3	0	0.031 ± 0.004	3	0
N-Nitrosoanatabine	149 ± 39	12	0	0.010 ± 0.002	3	0	0.015 ± 0.002	3	0	0.023 ± 0.001	3	0	0.040 ± 0.004	3	0	0.110 ± 0.006	3	0	0.250 ± 0.033	3	0	0.283 ± 0.039	3	0
N-Nitrosonornicotine	152 ± 58	12	0	0.01 ± 0.00	3	0	0.02 ± 0.00	3	0	0.02 ± 0.00	3	0	0.04 ± 0.00	3	0	0.11 ± 0.01	3	0	0.23 ± 0.03	3	0	0.27 ± 0.04	3	0
4-(Methylnitrosamino)-1-(3-pyridyl)-1-butanone (NNK)	97 ± 32	12	0	0.008 ± 0.001	3	0	0.011 ± 0.001	3	0	0.017 ± 0.001	3	0	0.029 ± 0.002	3	0	0.082 ± 0.006	3	0	0.185 ± 0.038	3	0	0.206 ± 0.024	3	0
Nornicotine	4430 ± 1270	12	0	0.3 ± 0.0	3	3	0.4 ± 0.0	3	3	0.5 ± 0.0	3	0	0.9 ± 0.1	3	0	2.1 ± 0.2	3	0	4.7 ± 0.1	3	0	4.9 ± 0.5	3	0
Phenanthrene	164 ± 54.2	12	0	0.0004 ± 0.0003	3	3	0.0003 ± 0.0003	3	3	0.0015 ± 0.0003	3	3	0.0024 ± 0.0014	3	2	0.0064 ± 0.0017	3	0	0 ± 0	3	3	0 ± 0	3	3
Pyrene	86 ± 24	12	0	0.0002 ± 0.0003	3	3	0 ± 0	3	3	0.0002 ± 0.0003	3	3	0.0002 ± 0.0001	3	3	0.0001 ± 0.0002	3	3	0 ± 0	3	3	0 ± 0	3	3
Solanesol	278,100 ± 110,200	12	0	0.06 ± 0.03	3	3	0.13 ± 0.08	3	1	0.15 ± 0.09	3	1	0.18 ± 0.10	3	1	0.50 ± 0.19	3	0	0.67 ± 0.03	3	0	0.77 ± 0.22	3	0
Thiophene	2370 ± 280	23	0	0.007 ± 0.003	4	4	0.007 ± 0.003	4	4	0.008 ± 0.003	4	4	0.010 ± 0.003	4	4	0.012 ± 0.003	4	4	0.021 ± 0.003	4	0	0.023 ± 0.002	4	0
Toluene	173,400 ± 31,600	23	0	0.05 ± 0.00	4	4	0.05 ± 0.00	4	4	0.07 ± 0.01	4	1	0.09 ± 0.01	4	0	0.15 ± 0.02	4	0	0.30 ± 0.05	4	0	0.37 ± 0.08	4	0

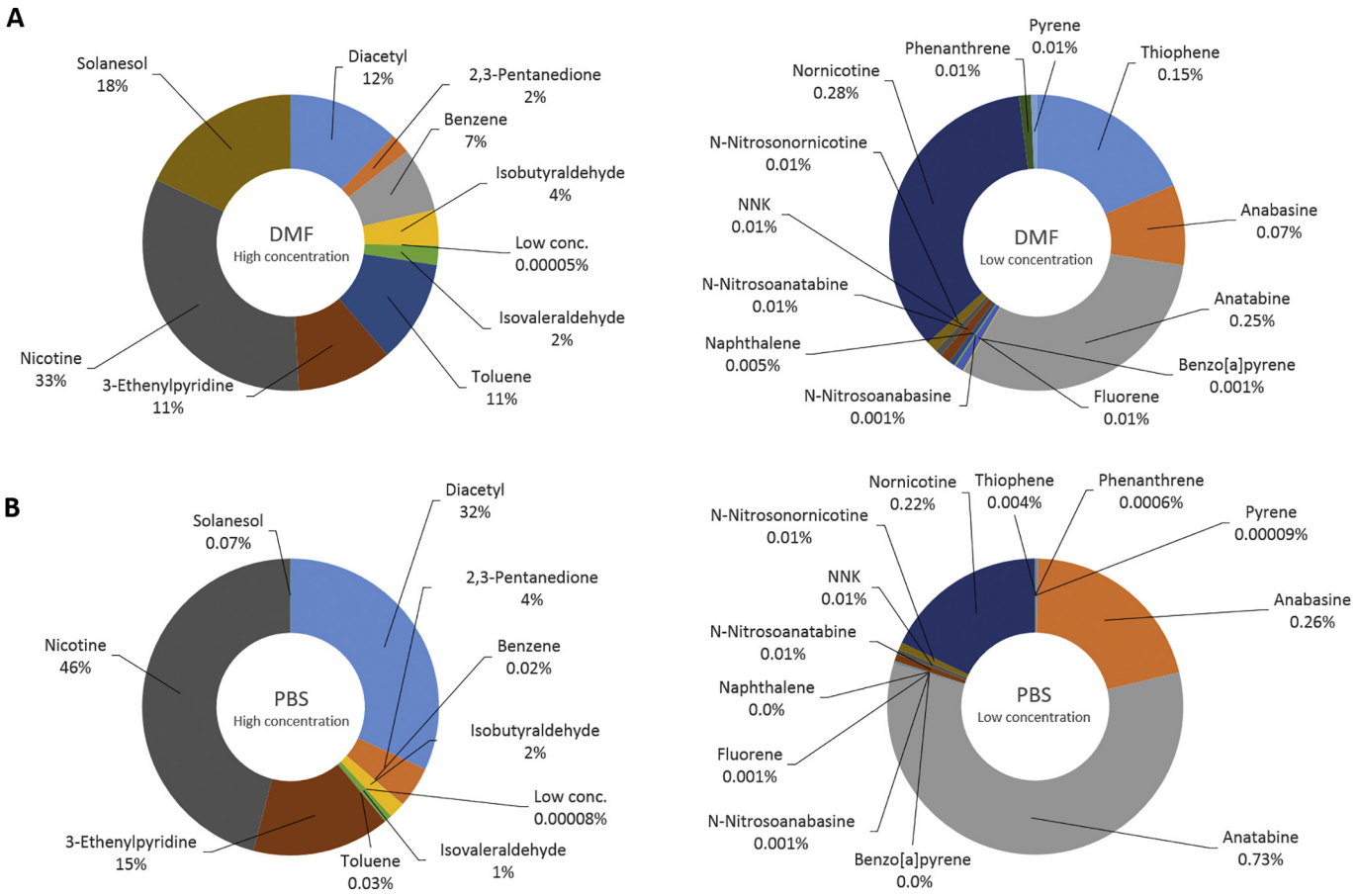

Fig. 2. Relative contribution of detected smoke constituents in A) the smoke in the dilution module of the VC24/48 system, as determined by trapping in DMF, and B) PBS following smoke exposure. Percentages were obtained by considering the sum of all detected masses as 100%. The listed percentages indicate the relative contribution of each of the 22 quantified smoke constituents to their cumulative mass (data obtained using a smoke concentration of 22%). The left and right diagrams separate the compounds present in high concentrations from the ones present in low concentrations (collectively shown as low conc. in the left diagrams).

not shown). PBS samples exposed only to air in rows 1 and 7 of the VC24/48 system (blank exposures) and DMF samples through which fresh air leaving the system was bubbled contained trace amounts of smoke constituents (data not shown), indicating system memory effects and carry-over between individual exposures. Compared with the amounts delivered during smoke exposures or trapped from complete smoke, this carry-over was negligible.

4. Discussion

The objective of the present work was the quantitative description of the conversion from applied dose to delivered dose during *in vitro* aerosol exposures, specifically for a complex, combustion-derived aerosol. For this purpose, the levels of smoke constituents detected in cigarette smoke and in smoke-exposed PBS samples were converted to compound-specific delivery efficiencies. These dimensionless values can be obtained using a non-targeted, semi quantitative, analytical approach, which greatly increases the number of compounds surveyed compared with the number covered by targeted approaches. In addition, these values are largely independent of the exact nature of the smoke and the absolute quantities of the compounds present, lending them a certain universal validity. To provide insight into absolute dosing and obtain an estimate of the performance of our sampling and analytical methods, absolute mass concentrations in the smoke and in the exposed PBS samples were also determined for a subset of 22 compounds.

Altogether, delivery efficiencies of 70 unambiguously identified constituents of 3R4F cigarette smoke could be described. Primarily, the differences between the delivery efficiencies of various compounds are of interest, as they describe the discrepancy between the composition of the applied dose and the delivered dose. These differences were of surprising magnitude (> 100,000-fold in some cases). A moderate example was provided by nicotine and toluene, two compounds with well-described bioactivity (*e.g.*, in the nervous system (Tormoehlen et al., 2014; Kobiella et al., 2014)). Both are relatively abundant in 3R4F smoke, and with nicotine being approximately three times more abundant in 3R4F smoke than toluene, their applied doses were comparable. However, they differed in their delivery efficiency by a factor of roughly 500, *i.e.*, once transferred into PBS, toluene was underrepresented roughly 500-fold if nicotine was used as the reference compound. Other compounds that were already present in very low amounts in the applied aerosol and that also displayed low delivery efficiencies (*e.g.*, benzo[*a*]pyrene) were virtually absent from the exposed liquid samples. In contrast, compounds such as acetonitrile or diacetyl were absorbed by the PBS with high efficiency, thereby contributing more to the delivered dose than to the applied dose.

The obvious implication is that biological responses to *in vitro* smoke exposures may not be fully attributable to the composition of the applied smoke. Although for complex aerosols such as cigarette smoke these attributions are commonly not possible, the experimental approach used here may be of interest when working with aerosols of lower complexity and controlled composition. For instance, in the process of developing inhalable consumer products and testing them *in vitro*, knowledge of the compound-specific delivery efficiencies may permit the identification of constituents that are overrepresented in the delivered dose and, accordingly, are likely to make a relevant

Table 2
Compound specific delivery efficiencies of 70 detected and unambiguously identified smoke constituents, for each constituent expressed in % of the mass present in the smoke at the inlet to the exposure chambers in the VC24/48. The compounds are sorted according to the average delivery efficiency obtained a 12–29% aerosol. Trapping efficiencies in DMF and delivery efficiencies corrected for the trapping efficiencies are included.

Compound	CAS #	Compound specific delivery efficiency (in %, at specified smoke concentration)										Structural properties			
		12%	17%	22%	29%	45%	67%	81%	Average delivery efficiency (12–29% smoke)	Trapping efficiency in DMF (according to Eq. (1))	Average delivery efficiency (12–29% smoke), corrected for trapping efficiency in DMF	Alkanes	Nitriles	Nitrosamines	Non-aromatic double bonds
Benzo[*a*]pyrene	50–32-8	0.0	0.0	0.0	0.0	1.1	0.0	1.2	0.0000	N/A	0.000				
Isoprene	78–79-5	0.0006	0.0005	0.0002	0.0002	0.0001	0.0001	0.0001	0.0004	95.2%	0.000				2
2-Butene-2-methyl	513–35-9	0.005	0.002	0.003	0.002	0.001	0.001	0.001	0.0028	87.7%	0.003				1
Cyclopentene	142–29-0	0.04	0.01	0.02	0.02	0.01	0.01	0.01	0.02	93.0%	0.022				1
2,5-Dimethylfuran	625–86-5	0.02	0.02	0.02	0.03	0.03	0.05	0.05	0.02	99.3%	0.023				
1,3-Butadiene	106–99-0	0.009	0.006	0.008	0.006	0.003	0.003	0.001	0.01	21.8%	0.033				2
2-Methylfuran	534–22-5	0.03	0.03	0.03	0.04	0.05	0.06	0.06	0.03	99.5%	0.033				
Toluene	108–88-3	0.05	0.04	0.04	0.04	0.04	0.05	0.06	0.04	99.5%	0.039				
1-Methylcyclopentene	693–89-0	0.07	0.04	0.02	0.03	0.01	0.01	0.01	0.04	98.3%	0.040				1
Solanesol	13,190–97-1	0.04	0.06	0.05	0.05	0.08	0.07	0.07	0.05	N/A	0.048				9
(E) 3-Methyl-2-pentene	616–12-6	0.10	0.03	0.02	0.04	0.02	0.03	0.02	0.05	97.1%	0.049				1
Benzene	71–43-2	0.05	0.05	0.05	0.05	0.06	0.08	0.07	0.05	99.4%	0.050				
Furan	110–00-9	0.06	0.03	0.05	0.07	0.05	0.09	0.08	0.05	N/A	0.051				
(E)-2-Pentene	646–04-8	0.05	0.04	0.04	0.02	0.03	0.01	0.03	0.04	55.5%	0.069				1
2-Ethylfuran	3208–16-0	0.06	N/A	0.12	0.03	0.23	0.15	0.07	0.07	99.0%	0.071				
2,3-Dimethylfuran	14,920–89-9	0.06	0.11	0.04	0.09	0.06	0.14	0.17	0.08	99.8%	0.076				
2,4-Dimethylfuran	3710–43-8	0.05	0.07	0.09	0.10	0.08	0.13	0.12	0.08	99.6%	0.078				
Carbon disulfide	75–15-0	0.13	0.02	0.04	0.04	0.05	0.04	0.01	0.06	73.1%	0.082				2

Compound	Structural properties									Physicochemical properties					
	Carbonyl compounds			Aromaticity											
	Esters	Ketones	Aldehydes	Fully aromatic molecules	Partly aromatic molecules	Monocyclic	Polycyclic	Heteroatoms in aromatic rings	Pyridine ring	Molar mass (g/mol)	Boiling point (°C at 1 atm)	LogP	Water solubility (mg/L at 25 °C)	Vapor pressure (mm Hg at 25 °C)	Polar surface area (Å^2)
Benzo[*a*]pyrene				x			5			252	475	6.1	0	5.50E-09	0
Isoprene										68	34	2.4	642	550	0
2-Butene-2-methyl										70	39	2.7	193	468	0
Cyclopentene										68	44	2.5	535	380	0
2,5-Dimethylfuran					x			O		96	94	2.2	1470	25.9	13
1,3-Butadiene										54	−4	2.0	735	2110	0
2-Methylfuran					x			O		82	65	1.9	3000	N/A	13
Toluene				x						92	111	2.7	526	28.4	0
1-Methylcyclopentene										82	76	3.0	N/A	N/A	0
Solanesol										631	N/A	N/A	N/A	N/A	20
(E) 3-Methyl-2-pentene										84	70	3.1	N/A	N/A	0
Benzene				x		x				78	80	2.1	1790	94.8	0
Furan				x		x		O		68	32	1.3	10,000	600	13
(E)-2-Pentene										70	36	2.6	203	506	0
2-Ethylfuran					x			O		96	92	2.4	1070	25.9	13
2,3-Dimethylfuran					x			O		96	N/A	N/A	N/A	N/A	13
2,4-Dimethylfuran					x			O		96	94	2.5	N/A	N/A	13
Carbon disulfide										76	46	1.9	2160	359	64

(*continued on next page*)

Table 2 (*continued*)

Compound	CAS #	Compound specific delivery efficiency (in %, at specified smoke concentration)										Structural properties			
		12%	17%	22%	29%	45%	67%	81%	Average delivery efficiency (12–29% smoke)	Trapping efficiency in DMF (according to Eq. (1))	Average delivery efficiency (12–29% smoke), corrected for trapping efficiency in DMF	Alkanes	Nitriles	Nitrosamines	Non-aromatic double bonds
Dimethyl disulfide	624–92-0	0.05	0.07	0.09	0.09	0.26	0.32	0.35	0.07	90.4%	0.082				
1-Hexene	592–41-6	0.11	0.08	0.07	0.12	0.12	0.10	0.13	0.10	95.1%	0.100				1
3-Methylfuran	930–27-8	0.13	0.09	0.11	0.13	0.15	0.25	0.20	0.11	99.3%	0.115				
2-Methylthiophene	554–14-3	0.17	0.17	0.11	0.12	0.14	0.16	0.19	0.14	99.7%	0.142				
Heptane	142–82-5	0.33	0.12	0.08	0.06	0.05	0.07	0.03	0.15	96.0%	0.155	x			
Cyclohexene	110–83-8	0.29	0.13	0.14	0.06	0.03	0.01	0.01	0.15	98.7%	0.157				1
Pyrene	129–00-0	0.30	0.03	0.24	0.14	0.08	0.00	0.00	0.18	N/A	0.177				
Octane	111–65-9	0.24	0.12	0.14	0.23	0.11	0.06	0.12	0.18	98.8%	0.186	x			
3-Methylthiophene	616–44-4	0.21	0.18	0.11	0.24	0.14	0.17	0.22	0.19	99.2%	0.189				
2-Methyl-2-hexene	2738–19-4	0.38	0.12	0.21	0.09	0.06	0.01	0.02	0.20	97.7%	0.206				1
1-Heptene	592–76-7	0.34	0.23	0.12	0.18	0.10	0.13	0.06	0.22	97.5%	0.222				1
2,3-Dimethyl-2-butene	563–79-1	0.64	0.14	0.24	0.08	0.30	0.28	0.11	0.27	95.5%	0.286				1
Thiophene	110–02-1	0.48	0.36	0.33	0.29	0.24	0.27	0.25	0.37	99.8%	0.367				
Phenanthrene	85–01-8	0.38	0.25	0.88	1.05	1.78	0.00	0.00	0.64	N/A	0.640				
Ethylenesulfide	420–12-2	0.23	0.81	0.73	1.1	1.3	1.8	1.7	0.71	99.7%	0.713				
Methylcyclopentane	96–37-7	0.44	0.86	1.17	0.50	0.50	0.30	0.49	0.74	95.5%	0.778	x			
Naphtalene	91–20-3	0.08	0.48	0	7.3	19	14.3	10.0	1.95	N/A	1.955				
Fluorene	86–73-7	1.3	1.5	2.8	2.9	4.0	5.4	4.3	2.13	N/A	2.134				

Compound	Structural properties								Physicochemical properties					
	Carbonyl compounds			Aromaticity										
	Esters	Ketones	Aldehydes	Fully aromatic molecules	Partly aromatic molecules	Monocyclic	Polycyclic	Heteroatoms in aromatic rings	Pyridine ring	Molar mass (g/mol)	Boiling point (°C at 1 atm)	LogP	Water solubility (mg/L at 25 °C)	Vapor pressure (mm Hg at 25 °C)	Polar surface area (Å^2)
Dimethyl disulfide										94	110	1.8	3000	28.7	51
1-Hexene										84	63	3.4	50	184	0
3-Methylfuran					x			O		82	66	1.9	3030	72.7	13
2-Methylthiophene					x			S		98	113	2.3	1210	24.9	28
Heptane										100	99	4.7	3	46	0
Cyclohexene										82	83	2.9	213	89	0
Pyrene				x			4			202	404	4.9	0	4.50E-06	0
Octane										114	126	5.2	1	14.1	0
3-Methylthiophene					x			S		98	116	2.3	400	22.2	28
2-Methyl-2-hexene										98	95	3.6	28	N/A	0
1-Heptene										98	94	4.0	18	59.3	0
2,3-Dimethyl-2-butene										84	73	3.2	71	126	0
Thiophene				x				S		84	84	1.8	3010	79.7	28
Phenanthrene				x			3			178	340	4.5	1	1.21E-04	0
Ethylenesulfide										60	56	0.8	28,100	250	25
Methylcyclopentane										84	72	3.4	42	138	0
Naphtalene				x			2			128	218	3.3	31	0.085	0
Fluorene				x			2			166	295	4.2	2	6.00E-04	0

(*continued on next page*)

Table 2 (*continued*)

Compound	CAS #	Compound specific delivery efficiency (in %, at specified smoke concentration)										Structural properties			
		12%	17%	22%	29%	45%	67%	81%	Average delivery efficiency (12–29% smoke)	Trapping efficiency in DMF (according to Eq. (1))	Average delivery efficiency (12–29% smoke), corrected for trapping efficiency in DMF	Alkanes	Nitriles	Nitrosamines	Non-aromatic double bonds
Isovaleraldehyde	590–86-3	6.7	6.0	5.7	6.2	7.0	9.2	8.3	6.15	98.9%	6.219				
Methyl-2-propenoate	96–33-3	5.5	5.6	6.4	8.3	11.0	15.3	13.8	6.45	98.4%	6.557				1
2-Methylbutanal	96–17-3	5.9	6.2	6.3	7.9	10.3	15.4	13.9	6.57	98.5%	6.667				
Isobutyraldehyde	78–84-2	6.5	6.5	6.5	7.5	9.4	12.7	10.8	6.74	98.3%	6.859				
1-Methyl-1H-pyrrole	96–54-8	6.5	6.4	6.7	8.7	10.1	14.3	15.5	7.09	100.0%	7.089				
Acrolein	107–02-8	8.2	7.4	7.8	9.2	10.3	11.7	9.2	8.16	99.3%	8.215				1
Methyl-isobutyl-ketone	108–10-1	6.2	7.5	7.0	10.7	11.5	15.1	16.7	7.85	93.3%	8.412				
3-Hexanone	589–38-8	7.7	8.8	8.1	10.0	11.8	16.2	21.2	8.62	N/A	8.619				
Methyl-isopropyl-ketone	563–80-4	11.4	8.9	8.9	10.8	15.0	23.4	20.5	9.98	98.7%	10.117				
N-Nitrosoanabasine	37,620–20-5	9.9	10.5	11.7	14.9	26.1	37.0	37.8	11.76	N/A	11.760			x	
Nornicotine	5746–86-1	9.8	11.8	11.3	14.4	21.2	32.5	28.4	11.82	N/A	11.817				
2-Methylbutanenitrile	18,936–17-9	11.2	11.2	10.5	14.5	15.9	21.2	23.6	11.85	98.9%	11.981		x		
Propanoic acid methyl ester	554–12-1	17.1	13.2	11.5	13.3	12.3	15.1	13.6	13.80	99.6%	13.848				
N-Nitrosonornicotine (NNN)	80,508–23-2	11.8	12.5	14.2	18.4	32.3	47.3	45.2	14.22	N/A	14.225			x	
N-Nitrosoanatabine	887,407–16-1	11.3	12.3	14.7	18.9	33.6	51.5	48.8	14.29	N/A	14.288			x	1
Acrylonitrile	107–13-1	13.0	13.4	13.1	17.7	21.8	29.8	25.5	14.31	99.9%	14.318		x		1
Butanal	123–72-8	13.9	15.4	16.2	18.5	25.4	36.3	30.9	15.98	N/A	15.977				
1-Penten-3-one	1629–58-9	16.2	14.4	13.5	20.3	25.9	34.1	31.7	16.11	99.9%	16.123				1

Compound	Structural properties									Physicochemical properties					
	Carbonyl compounds			Aromaticity											
	Esters	Ketones	Aldehydes	Fully aromatic molecules	Partly aromatic molecules	Monocyclic	Polycyclic	Heteroatoms in aromatic rings	Pyridine ring	Molar mass (g/mol)	Boiling point (°C at 1 atm)	LogP	Water solubility (mg/L at 25 °C)	Vapor pressure (mm Hg at 25 °C)	Polar surface area (Å^2)
Isovaleraldehyde			x							86	93	1.2	14,000	50	17
Methyl-2-propenoate	x									86	80	0.8	49,400	86.6	26
2-Methylbutanal			x							86	N/A	1.2	11,200	47.4	17
Isobutyraldehyde			x							72	65	0.7	89,000	173	17
1-Methyl-1H-pyrrole					x			N		81	115	1.2	12,100	21.4	5
Acrolein			x							56	53	−0.01	212,000	274	17
Methyl-isobutyl-ketone		1								100	117	1.3	19,000	19.9	17
3-Hexanone		1								100	124	1.2	14,700	13.9	17
Methyl-isopropyl-ketone		1								86	94	0.8	60,800	52.2	17
N-Nitrosoanabasine					x			N	x	191	N/A	N/A	N/A	N/A	46
Nornicotine					x			N	x	148	260	0.2	N/A	0.009	25
2-Methylbutanenitrile										83	125	1.1	8890	10.3	24
Propanoic acid methyl ester	x									88	80	0.8	62,400	84	26
N-Nitrosonornicotine (NNN)					x			N	x	177	N/A	0.3	N/A	5.10E-04	46
N-Nitrosoanatabine					x			N	x	189	N/A	N/A	N/A	N/A	46
Acrylonitrile										53	77	0.3	74,500	109	24
Butanal			x							72	75	0.9	71,000	111	17
1-Penten-3-one		1								84	N/A	N/A	N/A	N/A	17

Compound	CAS #	Compound specific delivery efficiency (in %, at specified smoke concentration)										Structural properties			
		12%	17%	22%	29%	45%	67%	81%	Average delivery efficiency (12–29% smoke)	Trapping efficiency in DMF (according to Eq. (1))	Average delivery efficiency (12–29% smoke), corrected for trapping efficiency in DMF	Alkanes	Nitriles	Nitrosamines	Non-aromatic double bonds
4-(Methylnitrosamino)-1-(3-pyridyl)-1-butanone (NNK)	64,091–91-4	13.6	14.0	16.3	20.9	38.5	58.3	54.4	16.20	N/A	16.196			x	
2-Methyl propanenitrile	78–82-0	15.2	15.9	14.6	20.4	23.9	31.4	28.1	16.53	98.5%	16.783		x		
2-Pentanone	107–87-9	12.2	11.7	10.7	15.2	17.5	25.4	24.1	12.44	72.7%	17.121				
Nicotine	22,083–74-5	25.1	16.7	20.0	24.1	40.7	87.5	79.3	21.47	N/A	21.471				
3-Ethenylpyridine	1121–55-7	25.9	16.7	20.6	23.9	38.2	71.7	69.2	21.77	N/A	21.771				1
Propionaldehyde	123–38-6	22.4	22.9	23.1	29.0	36.0	44.4	36.8	24.35	99.4%	24.504				
Crotonaldehyde	123–73-9	21.6	22.6	20.6	33.6	46.4	65.9	60.6	24.59	93.7%	26.255				1
3-Buten-2-one	78–94-4	28.7	25.4	26.8	39.0	52.6	73.9	57.5	29.96	98.6%	30.375				1
2,3-Pentanedione	600–14-6	27.7	29.6	28.8	33.6	44.3	54.7	40.2	29.93	98.4%	30.418				
Acetone	67–64-1	32.4	31.2	27.1	36.8	42.8	52.4	39.5	31.86	96.6%	32.970				
Propionitrile	107–12-0	35.0	36.4	31.7	47.3	59.5	78.1	62.4	37.59	99.9%	37.627		x		
Anatabine	2743–90-0	34.3	37.4	41.9	45.5	65.1	83.7	71.8	39.78	N/A	39.775				
Methylacetate	79–20-9	32.7	29.8	26.7	28.7	32.5	45.1	36.4	29.47	73.6%	40.049				
Diacetyl	431–03-8	47.9	44.5	37.5	49.6	62.6	71.8	50.3	44.87	99.8%	44.955				
Anabasine	13,078–04-1	36.6	42.0	52.5	56.7	96.6	123.7	98.4	46.96	N/A	46.955				
2-Butanone	78–93-3	37.7	37.8	33.9	49.6	65.8	92.5	74.4	39.76	82.2%	48.367				

Compound	Structural properties									Physicochemical properties					
	Carbonyl compounds			Aromaticity											
	Esters	Ketones	Aldehydes	Fully aromatic molecules	Partly aromatic molecules	Monocyclic	Polycyclic	Heteroatoms in aromatic rings	Pyridine ring	Molar mass (g/mol)	Boiling point (°C at 1 atm)	LogP	Water solubility (mg/L at 25 °C)	Vapor pressure (mm Hg at 25 °C)	Polar surface area (Å^2)
4-(Methylnitrosamino)-1-(3-pyridyl)-1-butanone (NNK)		1			x			N	x	207	N/A	0.0	103,000	6.80E-05	63
2-Methyl propanenitrile										69	104	0.5	55,000	32.7	24
2-Pentanone		1								86	102	0.9	43,000	35.4	17
Nicotine					x			N	x	162	247	1.2	1,000,000	0.038	16
3-Ethenylpyridine								N	x	105	162	1.7	N/A	N/A	13
Propionaldehyde			x							58	48	0.6	306,000	317	17
Crotonaldehyde			x							70	102	0.6	150,000	30	17
3-Buten-2-one		1								70	81	0.4	60,600	152	17
2,3-Pentanedione		2								100	108	−0.85	66,700	N/A	34
Acetone		1								58	56	−0.24	1,000,000	232	17
Propionitrile										55	97	0.2	103,000	47.4	24
Anatabine		1			x			N	x	160	N/A	N/A	N/A	N/A	25
Methylacetate	x									74	57	0.2	243,000	216	26
Diacetyl		2								86	88	−1.3	200,000	56.8	34
Anabasine					x			N	x	162	272	1.0	1,000,000	N/A	25
2-Butanone		1								72	80	0.3	223,000	90.6	17

contribution to the product's bioactivity *in vitro*. Evidently, as this example refers to aerosols of a considerably different nature than cigarette smoke, the validity of the delivery efficiencies reported here would have to be determined on a case-by-case basis.

Perhaps more interestingly, delivery efficiencies are useful for translating results of different exposure modes, such as between *in vitro* and *in vivo* work. A number of studies have reported the retention of cigarette smoke constituents in the human respiratory tract during smoking (Moldoveanu et al., 2007; Zhang et al., 2012; Baker and Dixon, 2006; Dalhamn et al., 1968; Armitage et al., 2004; Feng et al., 2007; McGrath et al., n.d.; Moldoveanu et al., 2008a; Moldoveanu et al., 2008b; Moldoveanu and Coleman III, 2008), and these retentions are the *in vivo* equivalent of the delivery efficiencies we report here. The comparison of delivery efficiencies with data on *in vivo* retention can yield a direct measure of how similar the composition of an *in vitro* delivered smoke fraction is to the *in vivo* retained fraction. If the ratio between the delivery efficiencies of two smoke constituents *in vitro* equals the ratio between their retention *in vivo*, the relative contribution of the two compounds to the overall smoke dose would be identical *in vitro* and *in vivo*.

Our findings reveal that the discrepancy between *in vitro* absorption and *in vivo* retention is large for some compounds. For toluene, for example, they differ by a factor of > 600 if the *in vivo* retention and the *in vitro* absorption of nicotine is used as a reference. For 14 out of the 20 compounds listed in Table 3, however, ratios far below 100 were obtained, and for eight of the compounds, the ratios were below 2. This indicates that i) for many smoke constituents, *in vivo* retention and *in vitro* absorption are in good agreement, but that ii) nevertheless, a direct translation of the biological impact of *in vitro* exposure to cigarette smoke to an *in vivo* situation may be biased. It furthermore indicates that differences between the acute biological response observed *in vitro* and *in vivo* cannot by implication be attributed to differences between the two biological test systems. When discussing the *in vitro* - *in vivo* comparison, we have to consider that, for the compounds displaying a > 100-fold discrepancy, we cannot rule out the use of a static, cell-free model such as PBS as a cause. PBS does not mimic all physicochemical properties of a cell culture surface and volume, and activities such as metabolism or transepithelial transport are absent from the PBS model. The diffusional equilibrium for some smoke constituents may therefore be shifted towards lower deposition compared with exposure conditions when using living cell cultures (although this would be visible in the results as saturation, which was not observed, at least not at the smoke concentrations on which our calculations are based (12%–29%)). Moreover, once in the PBS, hydrophobic compounds may have adsorbed to the polystyrene or polyethylene terephthalate surface of the cell culture inserts, thereby evading sampling and detection. Using an improved model of the liquid lining of cell cultures, such as artificial mucus, could improve the results, although this would still not account for the dynamic properties of cell cultures (metabolism and transport).

With the applied experimental design, we avoided the introduction of exposure system-specific effects such as the absorbance, condensation or sedimentation of smoke constituents at internal system surfaces, which in their magnitude are a function of the system's internal surface area, the material it is built of and the flow patterns; The characterization of the applied smoke was not conducted upstream of the system but rather in a location close to the exposure chambers, yet easily accessible for collecting large volumes of test aerosol for chemical characterization. It is important to note that what we refer to as the applied smoke is, as a consequence, not identical with the smoke that left the filter tip of the used reference cigarettes (as demonstrated by the discrepancy between the results of the smoke characterization reported here and literature values on 3R4F smoke composition), but the procedure bears the advantage that any difference in the composition of the smoke sampled for determining the applied and the delivered doses can be fully attributed to only three mechanisms: 1) unequal sampling of particles and gases and particles of different sizes into the exposure trumpets (Von der Weiden et al., 2009); 2) losses of smoke constituents at the inner surfaces of the exposure trumpets or the tubings connecting the impingers to the VC24/48; and 3) the delivery efficiency of the remaining smoke constituents across the liquid surface of the PBS samples. We consider the former two factors negligible; Firstly, size-selective particle sampling at the trumpet inlets has recently been shown to become relevant only if the size differences are in the micrometer range (Steiner et al., 2017b). Secondly significant adsorption of smoke constituents at the trumpet or tubing surfaces was not expected as the overall surface areas were small and the residence time of the smoke in the trumpets and the tubings was short.

Differences between the applied dose and the delivered dose are therefore largely the result of physical and chemical compound properties, the interactions between the compounds and the properties of the PBS and therefore can be considered as constant values describing processes during aerosol exposures at the air-liquid interface. As a consequence, if the delivery of a single aerosol constituent covered in this study is known under a given exposure setting (for instance nicotine delivery is frequently monitored as a marker compound in exposures to cigarette smoke), the delivery of other smoke constituents covered in this study can be estimated based on relative delivery efficiencies. Alternatively if no information on aerosol delivery is available at all, delivery efficiencies reported here may be used for estimating dose delivery based on the composition of the aerosol that is used for exposures: We suppose that in most aerosol exposure systems, locations equivalent to that of the dilution module in the VC24/48 system—close to the exposure chambers, yet easily accessible for sampling large test aerosol volumes during system operation—exist. Therefore, when information on the chemical composition of a test aerosol at such locations within other exposure systems is available, the delivery efficiencies reported here may allow the delivery of the 70 compounds we analyzed to be estimated, notably without the need for the more challenging and labor-intensive direct quantification in the exposed test samples. The requirements are that the exposure system consists of inert materials, is operated at 37 °C, at atmospheric pressure and high relative humidity, and relies on streaming the test aerosol over the biological test system at low flow velocities.

Evidently, the more comparable a test aerosol is to smoke generated from 3R4F cigarettes, and the more diluted it is, the more accurate such estimates will be. For the products of combustion of organic material (*e.g.* tobacco, wood, diesel, gasoline), we claim a certain universal validity of our results, as these aerosol types share a large fraction of their constituents (Schauer et al., 2002a; Khalili et al., 1995; Schauer et al., 2002b; Schauer et al., 1999; Schauer et al., 2001), hence can be expected to display comparable delivery patterns. For aerosols of highly different composition (*e.g.* deodorant or color sprays), although also sharing certain constituents with combustion products, the derived delivery efficiencies are unlikely to be valid.

Furthermore, because of the universal validity of the delivery efficiencies, we expected that sorting the compounds by their structural and/or physical properties should, to a certain degree, result in groupings with similar delivery efficiencies. This was indeed the case (Table 2): the lowest delivery efficiencies were seen for saturated and unsaturated hydrocarbons as well as for (partly or fully) aromatic compounds containing oxygen as heteroatoms in the aromatic ring system. The introduction of carbonyl groups resulted in a distinct, roughly three-fold increase in the delivery efficiencies, whereby keto-groups appear to have a stronger effect than aldo-groups. Aldehydes commonly did not reach delivery efficiencies higher than 25%, whereas ketones were among the most efficiently delivered compounds detected. A group of compounds that can be categorized as a nitrile or pyridine ring-containing group (all detected nitriles, nicotine, nornicotine, anabasine, anatabine, and the corresponding nitrosamines) exhibited delivery efficiencies within the range seen for ketones. Notably, within this group, nitrosamines consistently displayed the lowest

Table 3
In vitro delivery efficiencies measured in this work and *in vivo* retention of cigarette smoke constituents as reported in various publications. If the literature reports ranges of retention, these are indicated followed by the reported average in brackets. The lower section of the table shows *in vitro* delivery efficiencies and *in vivo* retentions and the relative contribution of the compounds to the *in vivo* retained smoke fraction compared to the *in vitro* delivered smoke fraction, with nicotine as reference compound (in each case with nicotine as reference compound).

	1,3-Butadiene	2-Butanone	2-Pentanone	Acetone	Acroleine	Benzo[a]pyrene	Benzene	Butanal	Fluorene	Isoprene	Isovaleraldehyde	Naphthalene	Nicotine	NNK	NNN	Phenanthrene	Propionaldehyde	Propionitrile	Pyrene	Solanesol	Toluene
In vitro transfer efficiency (%)	0.01	40	12	32	8	0	0.05	16	2	0.0004	6	1.95	21	16	14	0.64	24	37	0.2	0.05	0.04
In vivo retention (%) Moldoveanu et al. 2007 [37]				92.6	99.7			98.7									98				
Zhang et al. 2012 [38]	<5				98																
Baker et al. 2006 [39]		82	82	76	97		75			49	94		50 - 100 (79)					71			92
Dalhamn et al. 1968 [40]				86						99											96
Armitage et al. 2004 [41]													99							71	
Feng et al. 2007 [42]										50			>98	84	97						
McGrath et al. 2009 [43]													20 - 67 (47)								
Moldoveanu et al. 2008 [44]							89 - 98 (94)														87 - 99 (94)
Moldoveanu et al. 2008 [45]						71			98			97				95			93		
Moldoveanu et al. 2008 [46]																				60 - 72 (66)	
Average *in vitro* transfer efficiency, normalized to nicotine	0.0005	1.9	0.6	1.5	0.4	0	0.0024	0.8	0.10	0.00002	0.3	0.09	1	0.8	0.7	0.03	1.1	1.8	0.0095	0.0024	0.0019
Average *in vivo* retention, normalized to nicotine	0.1	1.0	1.0	1.1	1.2	0.9	1.2	1.2	1.2	0.8	1.2	1.2	1	1.0	1.2	1.2	1.2	0.9	1.2	0.8	1.2
Ratio *in vivo* / *in vitro* (Reference: nicotine)	**130**	**0.5**	**1.8**	**0.7**	**3.2**	**N/D**	**489**	**1.6**	**13**	**42910**	**4.1**	**13**	**1**	**1.4**	**1.8**	**39**	**1.1**	**0.5**	**121**	**356**	**611**

delivery efficiencies.

Similarly, sorting aerosol constituents by their delivery efficiencies resulted in groupings by some of their physical properties. For instance, a delivery efficiency of 6% or higher was only reached for compounds with a polar surface area higher than 20 $Å^2$, unless sulfur was present in the molecule. Qualitatively, groupings were also observed by water solubility and by the water-octanol partition coefficient (LogP), although several exceptions were detected for the water solubility groupings (low delivery efficiency and high water solubility), interestingly all containing either sulfur or oxygen atoms. A distinct sorting of other physicochemical parameters listed in Table 2 (*i.e.*, the molecular mass, the boiling point, and the vapor pressure) was not evident at first glance, but a multiparameter analysis may reveal other patterns.

These observations may therefore lead to the development of multivariate models that can predict delivery efficiencies from the chemical structures and/or physical properties of the compounds. Determining whether such models can be designed and whether they would be universally valid or limited to aerosols or gases of specific origin presents an interesting topic for further research.

5. Conclusions

We provide a large set of delivery efficiencies that describe the conversion of an applied dose of cigarette smoke to a delivered dose during *in vitro* exposure. These delivery efficiencies provide a simple dose metric tool that allows the characterization and comparison of aerosol exposure experiments with respect to the composition of the aerosol presented to the biological test system.

We demonstrated that the efficiency with which different chemical compounds present in cigarette smoke are transferred across an aqueous liquid surface may vary by several orders of magnitude and that consequently, characterization of the smoke used in *in vitro* exposures does not necessarily give an accurate description of the smoke fraction that ultimately enters and interacts with the biological test system. Furthermore, we noted the potential bias which may occur when translating the results of *in vitro* exposures to *in vivo* smoke toxicity.

Owing to the nature of the delivery efficiencies and the applied experimental design, the presented results are of little specificity to the model aerosol and exposure system used. Rather, our results are likely generalizable to a variety of aerosol exposure systems and a variety of aerosols. Moreover, as the measured delivery efficiencies correlated with the structural and physicochemical properties of the compounds, the development of a predictive tool for calculating delivery efficiencies of compounds not covered in this work appears feasible and will be explored further.

Transparency document

The Transparency document associated to this article can be found, in the online version.

Appendix A. Supplementary data

Supplementary data to this article can be found online at https://doi.org/10.1016/j.tiv.2018.06.024.

References

Adam, G., Läuger, P., Stark, G., 2009. Physikalische chemie und biophysik. Springer-Verlag.

Armitage, A., Dixon, M., Frost, B., Mariner, D., Sinclair, N., 2004. The effect of inhalation volume and breath-hold duration on the retention of nicotine and solanesol in the human respiratory tract and on subsequent plasma nicotine concentrations during cigarette smoking. Contrib. Tobacco Res. 21 (4), 240–249.

Atkin, P., de Paula, J., 2006. Atkins' Physical Chemistry. WH Freeman and Company Books, pp. 747–755.

Baker, R.R., Dixon, M., 2006. The retention of tobacco smoke constituents in the human respiratory tract. Inhal. Toxicol. 18 (4), 255–294.

Bodnar, J., Morgan, W., Murphy, P., Ogden, M., 2012. Mainstream smoke chemistry analysis of samples from the 2009 US cigarette market. Regul. Toxicol. Pharmacol. 64 (1), 35–42.

Breheny, D., Cunningham, F., Kilford, J., Payne, R., Dillon, D., Meredith, C., 2014. Application of a modified gaseous exposure system to the in vitro toxicological assessment of tobacco smoke toxicants. Environ. Mol. Mutagen. 55 (8), 662–672.

Burch, R.L., WMS, Russel (Eds.), 1959. The Principles of Humane Experimental Technique.

Dalhamn, T., Edfors, M.-L., Rylander, R., 1968. Retention of cigarette smoke components in human lungs. Archiv. Environ. Health 17 (5), 746–748.

Davidovits, P., Kolb, C.E., Williams, L.R., Jayne, J.T., Worsnop, D.R., 2006. Mass accommodation and chemical reactions at gas− liquid interfaces. Chem. Rev. 106 (4), 1323–1354.

Dong, J.-Z., Moldoveanu, S.C., 2004. Gas chromatography–mass spectrometry of carbonyl compounds in cigarette mainstream smoke after derivatization with 2,4-dinitrophenylhydrazine. J. Chromatogr. A 1027 (1), 25–35. https://doi.org/10.1016/j.chroma.2003.08.104.

Dossin, E., Martin, E., Diana, P., Castellon, A., Monge, A., Pospisil, P., et al., 2016. Prediction models of retention indices for increased confidence in structural elucidation during complex matrix analysis: application to gas chromatography coupled with high-resolution mass spectrometry. Anal. Chem. 88 (15), 7539–7547.

Eldridge, A., Betson, T., Gama, M.V., McAdam, K., 2015. Variation in tobacco and mainstream smoke toxicant yields from selected commercial cigarette products. Regul. Toxicol. Pharmacol. 71 (3), 409–427.

Feng, S., Plunkett, S.E., Lam, K., Kapur, S., Muhammad, R., Jin, Y., et al., 2007. A new method for estimating the retention of selected smoke constituents in the respiratory tract of smokers during cigarette smoking. Inhal. Toxicol. 19 (2), 169–179.

Forehand, J., Dooly, G., Moldoveanu, S., 2000. Analysis of polycyclic aromatic hydrocarbons, phenols and aromatic amines in particulate phase cigarette smoke using simultaneous distillation and extraction as a sole sample clean-up step. J. Chromatogr. A 898 (1), 111–124.

Fröhlich, E., Bonstingl, G., Höfler, A., Meindl, C., Leitinger, G., Pieber, T.R., et al., 2013. Comparison of two in vitro systems to assess cellular effects of nanoparticles-containing aerosols. Toxicol. in Vitro 27 (1), 409–417.

Harper, M., 2000. Sorbent trapping of volatile organic compounds from air. J. Chromatogr. A 885 (1), 129–151. https://doi.org/10.1016/S0021-9673(00)00363-0.

Johansen, I., Wendelboe, J.F., 1981. Dimethylformamide and carbon disulphide desorption efficiencies for organic vapours on gas-sampling charcoal tube analyses with a gas chromatographic backflush technique. J. Chromatogr. A 217 (Suppl. C), 317–326. https://doi.org/10.1016/S0021-9673(00)88086-3.

Kaur, N., Lacasse, M., Roy, J.-P., Cabral, J.-L., Adamson, J., Errington, G., et al., 2010. Evaluation of precision and accuracy of the Borgwaldt RM20S® smoking machine designed for in vitro exposure. Inhal. Toxicol. 22 (14), 1174–1183.

Kaur, N., Cabral, J.-L., Morin, A., Waldron, K.C., 2011. Headspace stir bar sorptive extraction–gas chromatography/mass spectrometry characterization of the diluted vapor phase of cigarette smoke delivered to an in vitro cell exposure chamber. J. Chromatogr. A 1218 (2), 324–333.

Khalili, N.R., Scheff, P.A., Holsen, T.M., 1995. PAH source fingerprints for coke ovens, diesel and, gasoline engines, highway tunnels, and wood combustion emissions. Atmos. Environ. 29 (4), 533–542.

Kobiella, A., Ripke, S., Kroemer, N.B., Vollmert, C., Vollstädt-Klein, S., Ulshöfer, D.E., et al., 2014. Acute and chronic nicotine effects on behaviour and brain activation during intertemporal decision making. Addict. Biol. 19 (5), 918–930.

Kumar, S., Nayek, M., Kumar, A., Tandon, A., Mondal, P., Vijay, P., et al., 2011. Aldehyde, ketone and methane emissions from motor vehicle exhaust: a critical review. Am. Chem. Sci. J. 1 (1), 1–27.

Leonard, R.E., Kiefer, J.E., 1966. Quantitative determination of formaldehyde in gross impure mixtures containing other carbonyl compounds. J. Chromatogr. Sci. 4 (4), 142–143. https://doi.org/10.1093/chromsci/4.4.142.

Li, X., 2016. In vitro toxicity testing of cigarette smoke based on the air-liquid interface exposure: a review. Toxicol. in Vitro 36, 105–113.

Liu, C., Feng, S., Van Heemst, J., McAdam, K., 2010. New insights into the formation of volatile compounds in mainstream cigarette smoke. Anal. Bioanal. Chem. 396 (5), 1817–1830.

Majeed, S., Frentzel, S., Wagner, S., Kuehn, D., Leroy, P., Guy, P.A., et al., 2014. Characterization of the Vitrocell® 24/48 in vitro aerosol exposure system using mainstream cigarette smoke. Chem. Central J. 8 (1), 62. https://doi.org/10.1186/s13065-014-0062-3.

Marcilla, A., Beltran, M., Gómez-Siurana, A., Berenguer, D., Martínez-Castellanos, I., 2014. Comparison between the mainstream smoke of eleven RYO tobacco brands and the reference tobacco 3R4F. Toxicol. Rep. 1, 122–136.

McGrath C, Warren N, Biggs P, McAughey J: Real-time measurement of inhaled and exhaled cigarette smoke: Implications for dose. In: Journal of Physics: Conference Series2009: IOP Publishing: 012018.

Moldoveanu, S.C., Coleman III, W., 2008. A pilot study to assess solanesol levels in exhaled cigarette smoke. Contrib. Tobacco Res. 23 (3), 144–152.

Moldoveanu, S., Coleman, W., Wilkins, J., 2007. Determination of carbonyl compounds in exhaled cigarette smoke. Contrib. Tobacco Res. 22 (5), 346–357.

Moldoveanu, S., Coleman, I.I.I.W., Wilkins, J., 2008a. Determination of benzene and toluene in exhaled cigarette smoke. Contrib. Tob. Res. 23 (2), 107–114.

Moldoveanu, S.C., Coleman III, W., Wilkins, J.M., 2008b. Determination of polycyclic aromatic hydrocarbons in exhaled cigarette smoke. Contrib. Tobacco Res. 23 (2), 85–97.

Muller, L., Gasser, M., Raemy, D.O., Herzog, F., Brandenberger, C., Schmid, O., et al., 2011. Realistic exposure methods for investigating the interaction of nanoparticles with the lung at the air-liquid Interface in vitro. Insci. J. 1 (1), 30–64. https://doi.

org/10.5640/insc.010130.
Muller, L., Comte, P., Czerwinski, J., Kasper, M., Mayer, A.C.R., Schmid, A., et al., 2012. Investigating the potential for different scooter and car exhaust emissions to cause cytotoxic and (pro-)inflammatory responses to a 3D in vitro model of the human epithelial airway. Toxicol. Environ. Chem. 94 (1), 164–180. https://doi.org/10.1080/02772248.2011.632509. < Go to ISI > ://000302596800017.
Pankow, J.F., 2001. A consideration of the role of gas/particle partitioning in the deposition of nicotine and other tobacco smoke compounds in the respiratory tract. Chem. Res. Toxicol. 14 (11), 1465–1481.
Paschke, T., Scherer, G., Heller, W.-D., 2014. Effects of ingredients on cigarette smoke composition and biological activity: a literature overview. Contrib. Tob. Res. 20 (3), 107–247.
Paur, H.R., Mulhopt, S., Weiss, C., Diabate, S., 2008. In vitro exposure systems and bioassays for the assessment of toxicity of nanoparticles to the human lung. J Verbrauch Lebensm. 3 (3), 319–329. https://doi.org/10.1007/s00003-008-0356-2. (< Go to ISI > ://000258903600012).
Paur, H.R., Cassee, F.R., Teeguarden, J., Fissan, H., Diabate, S., Aufderheide, M., et al., 2011. In-vitro cell exposure studies for the assessment of nanoparticle toxicity in the lung-A dialog between aerosol science and biology. J. Aerosol. Sci. 42 (10), 668–692. https://doi.org/10.1016/j.jaerosci.2011.06.005. (< Go to ISI > ://000294572600005).
Perfetti, T.A., Rodgman, A., 2011. The complexity of tobacco and tobacco smoke. Contrib. Tobacco Res. 24 (5), 215–232.
Purkis, S.W., Meger, M., Wuttke, R., 2012. A review of current smoke constituent measurement activities and aspects of yield variability. Regul. Toxicol. Pharmacol. 62 (1), 202–213.
Sarigiannis, D.A., Karakitsios, S.P., Gotti, A., Liakos, I.L., Katsoyiannis, A., 2011. Exposure to major volatile organic compounds and carbonyls in European indoor environments and associated health risk. Environ. Int. 37 (4), 743–765.
Schauer, J.J., Kleeman, M.J., Cass, G.R., Simoneit, B.R., 1999. Measurement of emissions from air pollution sources. 2. C1 through C30 organic compounds from medium duty diesel trucks. Environ. Sci. Technol. 33 (10), 1578–1587.
Schauer, J.J., Kleeman, M.J., Cass, G.R., Simoneit, B.R., 2001. Measurement of emissions from air pollution sources. 3. C1 − C29 organic compounds from fireplace combustion of wood. Environ. Sci. Technol. 35 (9), 1716–1728.
Schauer, J.J., Kleeman, M.J., Cass, G.R., Simoneit, B.R., 2002a. Measurement of emissions from air pollution sources. 4. C1 − C27 organic compounds from cooking with seed oils. Environ. Sci. Technol. 36 (4), 567–575.
Schauer, J.J., Kleeman, M.J., Cass, G.R., Simoneit, B.R., 2002b. Measurement of emissions from air pollution sources. 5. C1 − C32 organic compounds from gasoline-powered motor vehicles. Environ. Sci. Technol. 36 (6), 1169–1180.
Scian, M.J., Oldham, M.J., Miller, J.H., Kane, D.B., Edmiston, J.S., McKinney, W.J., 2009. Chemical analysis of cigarette smoke particulate generated in the MSB-01 in vitro whole smoke exposure system. Inhal. Toxicol. 21 (12), 1040–1052.
Shahir, V., Jawahar, C., Suresh, P., 2015. Comparative study of diesel and biodiesel on CI engine with emphasis to emissions—a review. Renew. Sust. Energ. Rev. 45, 686–697.
Shamir, E.R., Ewald, A.J., 2014. Three-dimensional organotypic culture: experimental models of mammalian biology and disease. Nat. Rev. Mol. Cell Biol. 15 (10), 647–664.
Steiner, S., Majeed, S., Kratzer, G., Vuillaume, G., Hoeng, J., Frentzel, S., 2017a. Characterization of the Vitrocell® 24/48 aerosol exposure system for its use in exposures to liquid aerosols. Toxicol. in Vitro 42, 263–272.
Steiner, S., Majeed, S., Kratzer, G., Hoeng, J., Frentzel, S., 2017b. A new fluorescence-based method for characterizing in vitro aerosol exposure systems. Toxicol. in Vitro 38, 150–158.
Teeguarden, J.G., Hinderliter, P.M., Orr, G., Thrall, B.D., Pounds, J.G., 2006. Particokinetics in vitro: dosimetry considerations for in vitro nanoparticle toxicity assessments. Toxicol. Sci. 95 (2), 300–312.
Thorne, D., Adamson, J., 2013. A review of in vitro cigarette smoke exposure systems. Exp. Toxicol. Pathol. 65 (7), 1183–1193.
Tippe, A., Heinzmann, U., Roth, C., 2002. Deposition of fine and ultrafine aerosol particles during exposure at the air/cell interface. J. Aerosol Sci. 33 (2), 207–218.
Tormoehlen, L., Tekulve, K., Nanagas, K., 2014. Hydrocarbon toxicity: a review. Clin. Toxicol. 52 (5), 479–489.
Von der Weiden, S., Drewnick, F., Borrmann, S., 2009. Particle Loss Calculator–a new software tool for the assessment of the performance of aerosol inlet systems. Atmos. Meas. Tech. 2 (2), 479–494.
www.vitrocell.com.
Zhang, Z., Kleinstreuer, C., Feng, Y., 2012. Vapor deposition during cigarette smoke inhalation in a subject-specific human airway model. J. Aerosol Sci. 53, 40–60.